Analyst

Accepted Manuscript

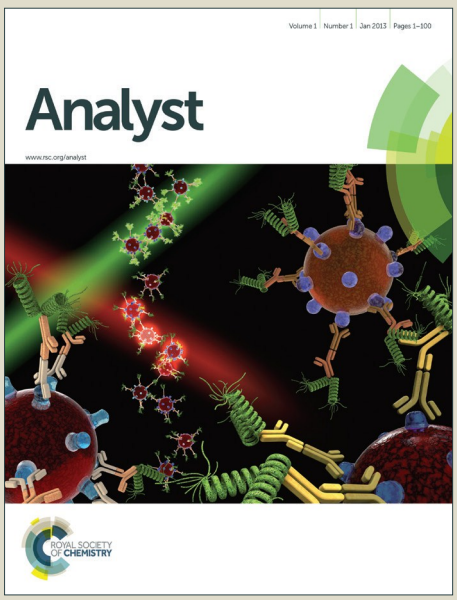

This is an *Accepted Manuscript*, which has been through the Royal Society of Chemistry peer review process and has been accepted for publication.

Accepted Manuscripts are published online shortly after acceptance, before technical editing, formatting and proof reading. Using this free service, authors can make their results available to the community, in citable form, before we publish the edited article. We will replace this *Accepted Manuscript* with the edited and formatted *Advance Article* as soon as it is available.

You can find more information about *Accepted Manuscripts* in the Information for Authors.

Please note that technical editing may introduce minor changes to the text and/or graphics, which may alter content. The journal's standard Terms & Conditions and the Ethical guidelines still apply. In no event shall the Royal Society of Chemistry be held responsible for any errors or omissions in this *Accepted Manuscript* or any consequences arising from the use of any information it contains.

ROYAL SOCIETY OF CHEMISTRY

www.rsc.org/analyst

Please do not adjust margins

Analyst

ARTICLE

Chemically modified graphene films for high-performance optical NO_2 sensors†

Received 00th January 20xx,
Accepted 00th January 20xx

DOI: 10.1039/x0xx00000x

www.rsc.org

Fei Xing,[a] Shan Zhang,[a] Yong Yang,*[b] Wenshuai Jiang,[c] Zhibo Liu,[c] Siwei Zhu[d] and Xiaocong Yuan*[a]

Various graphene-based gas sensors that operate based on the electrical properties of graphene have been developed for accurate detection of gas components. However, electronic graphene-based gas sensors are unsafe in explosive atmospheres and sensitive to electromagnetic interference. Here, a novel optical graphene-based gas sensor for NO_2 detection is established based on surface chemical modification of high-temperature-reduced graphene oxide (h-rGO) films with sulfo groups. Sulfo group-modified h-rGO (S-h-rGO) films with a thickness of several nanometers exhibit excellent performance in NO_2 detection at room temperature and atmospheric pressure based on the polarization absorption effect of graphene. Initial slope analysis of the S-h-rGO sensor indicates that it has a limit of detection of 0.28 ppm and response time of 300 s for NO_2 gas sensing. Furthermore, the S-h-rGO sensor also possesses the advantages of good linearity, reversibility, selectivity, non-contact operation, low cost and safety. This novel optical gas sensor has the potential to serve as a general platform for the selective detection of a variety of gases with high performance.

Introduction

Fast and accurate detection of harmful,[1, 2] toxic,[3,4] combustible and explosive[5,6] gases is required to avoid personal injury and monitor environmental pollution. Graphene, a truly two-dimensional material, exhibits distinct advantages for accurate gas detection at room temperature, including sensitive surface electronic structure, easy chemical modification, and repeated usage without surface contamination.[7-10] In 2007, Novoselov and co-workers reported a pioneering sensor for detecting single gas molecules based on the electrical properties of graphene.[7] Inspired by this work, various graphene-based materials have been developed for electrical gas sensing, including graphene prepared by mechanical exfoliation,[11-13] epitaxial growth,[14] and chemical vapor deposition,[15,16] along with reduced graphene oxide (rGO) and chemically modified rGO.[17-23] In particular, chemically modified rGO materials have attracted great attention because of their ability to realize selective, reversible gas flow sensing at low cost with the possibility of large-scale production.[18, 20-23] However, to enhance the sensitivity of electronic sensors, the gas-permeation properties of the whole graphene-based sensing layer need to be preserved to increase the available specific surface area,[20,22,23] which inevitably sacrifices the response time because of the need for internal gas adsorption. Moreover, the use of electronic gas sensors in certain environments, remote places, potentially explosive atmospheres and areas with high electromagnetic interference is either difficult or impossible.[24] Optical detection methods can overcome these deficiencies of electronic sensors.[25-27] However, traditional optical methods require high-precision instruments,[25-26] and carefully controlled conditions.[27] These limitations may be addressed by suitable combination of chemically modified graphene materials and a novel optical measurement method.

High-performance optial gas sensors should have the advantages of high sensitivity and resolution, fast response and recovery times, good linearity, reversibility and selectivity. Here, we report a novel optical NO_2 gas sensor based on a high-temperature-reduced graphene oxide (h-rGO) film chemically modified with sulfo groups. The detection principle of this sensor is based on the polarization absorption effect of graphene first found by us.[28-31] The sulfo group-modified h-rGO (S-h-rGO) film with a thickness of several nanometers exhibits excellent performance in NO_2 detection at room temperature and atmospheric pressure. The sensitivity and resolution of the S-h-rGO sensor are 78 mV/ppm and 0.77 ppm based on maximum response analysis method. In addition, the S-h-rGO sensor has good linearity, reversibility and selectivity. Because of the advantages of surface chemical modification, particularly impermeable adsorption and exchange of gas molecules, we propose an initial slope analysis method. Based on the initial slope analysis method, the resolution of the S-h-rGO sensor is up to 0.28 ppm; the issues caused by the inverse relationship between sensitivity and response time in the saturated response analysis method were solved, and response time is shortened to 300 s. The

[a] Institute of Micro & Nano Optics, Key Laboratory of Optoelectronic Devices and Systems of Ministry of Education and Guangdong Province, College of Optoelectronic Engineering, Shenzhen University, Shenzhen, 518060, P.R. China; xcyuan@szu.edu.cn
[b] Institute of Modern Optics, Key Laboratory of Optoelectronic Information Science & Technology, Ministry of Education of China, Nankai University, Tianjin, 300071, P.R. China; yangyong@nankai.edu.cn
[c] Key Laboratory of Weak Light Nonlinear Photonics, Ministry of Education, Teda Applied Physics School and School of Physics, Nankai University, Tianjin 300457, P.R. China
[d] Institute of Oncology, Tianjin Union Medicine Centre, Tianjin, 300121, P.R. China
† Electronic Supplementary Information (ESI) available: Table S1 and Figure S1. See DOI: 10.1039/x0xx00000x

Analyst Accepted Manuscript

Please do not adjust margins

initial slope analysis method is expected to become a general analysis method for surface gas sensors.

Experimental

Fabrication of GO and h-rGO films

Graphene oxide (GO) was prepared from graphite by the modified Hummers' method, and was used as the starting material to fabricate high-quality graphene films following a reported procedure.[32,33] Pre-cleaned quartz substrates were treated with oxygen plasma (Harrick Plasma, America) for 1 min prior to use. Typically, a 5 mg/mL GO dispersion in water was spin-coated on the quartz surfaces at 2000 rpm for 45 s. The resulting supported GO films were then thermally annealed at 950 °C for 1 hour in a mixed atmosphere of 95% N_2 and 5% H_2 gases (by volume) to obtain h-rGO films.

Fabrication of S-h-rGO films

S-h-rGO films were fabricated by the modified sulfonated graphene method[23, 34] as follows. First, h-rGO films were treated with oxygen plasma for 3 s to activate their surfaces. An aryl diazonium salt was prepared by the reaction of sulfanilic acid and sodium nitrite in HCl solution in an ice bath. The surface-activated h-rGO films were placed in the diazonium salt solution and kept in an ice bath for 2 h. After rinsing with deionized water several times and drying under a N_2 stream, the S-h-rGO films were obtained.

Fabrication of sensors

The sensor consisted of a polydimethylsiloxane (PDMS) gas cell, S-h-rGO (h-rGO) film and prism. The PDMS gas cell was fabricated according to the literature[35] as follows. A PDMS pre-polymer mixture of silicone elastomer base (Sylgard 184, 100 g) and elastomer curing agent (10 g, 10:1 ratio) was placed on a vacuum line in a fume hood for 1 h to trap any bubbles. The liquid mixture was then poured on a mold. The dish containing both the mold and PDMS pre-polymer was placed in an oven set to 70 °C and cured for 3 h. The solidified PDMS gas cell was then peeled off the mold. A pre-cleaned prism and PDMS gas cell were cleaned in oxygen plasma at 150 W for 50 s, and densely cross-linked surface on the PDMS gas cell was formed[36, 37], which can significantly block gas absorption. After dropping matching liquid between the S-h-rGO (h-rGO) film/quartz substrate and prism, the PDMS gas cell was irreversibly adhered to the prism to form a structure of PDMS gas cell/S-h-rGO (h-rGO) film/quartz substrate/prism.

Experimental setup

Light from a 632.8-nm He-Ne laser (Melles Griot, America) was adjusted to circularly polarized using a polarizer and quarter-wave plate. A neutral density filter was used to control the laser power. The light was incident in the center of the optical sensing element. Then, the reflected transverse electric (TE) and transverse magnetic (TM) modes were separated by a polarization beam splitter and monitored with a balanced detector (Thorlabs, PDB210A).

To accurately measure the concentration of NO_2 molecules, a carefully designed gas system was used to precisely control molecular concentration at atmospheric pressure. During the experiment, a continuous gas flow with a controlled concentration and low speed was provided to the system to minimize the change of concentration of the upper gas molecules. An optical sensing element was designed for the target gas sensing application that consisted of a PDMS gas cell, S-h-rGO film and prism.

Characterization

X-ray photoelectron spectroscopy (XPS) was measured using an AXIS Ultra DLD spectrometer (Kratos, Japan). A micro Raman spectrometer (Renishaw, RM2000) was used to acquire Raman spectra. A 514-nm excitation laser was used in the Raman measurements. Atomic force microscopy (AFM) was performed using a Dimension 3100 microscope (Veeco, America) in tapping mode at a scan rate of 1.003 Hz. The resonant frequency and force constant of the cantilever were 300 kHz and 40 N/m, respectively.

Results and discussion

Characterization of h-rGO and S-h-rGO films

GO aqueous solution and h-rGO films were fabricated according to previous reports,[28,32,33] and S-h-rGO films were fabricated by a modified graphene sulfonation method.[23,34] The compositions of h-rGO and S-h-rGO films were determined by XPS. Fig. 1a shows the XPS characteristics of a h-rGO film, indicating that it is composed of the elements C, O, and Si. The characteristic peaks of Si originated from the silica substrate, which demonstrates that the X-ray passed through the whole film during XPS characterization. In the XPS curve of the S-h-rGO film in Fig. 1b, the characteristic peak of S was detected in addition to the elements C, O, and Si. Fig. 1c depicts a high-resolution narrow scan of the S region of the S-h-rGO film, revealing the S signal is at ~168.5 eV. This indicates that S is hexavalent, which is consistent with the surface of the h-rGO film being successfully modified with sulfo groups. Quantitative analysis indicated that the C/S and C/O atomic ratios of the S-h-rGO film were 141.7 and 11.9, respectively (see Supplementary Information, Table S1). The content of S atoms is low, and only the surface of the h-rGO film (about 1–2 nm deep) is modified with S. Thus, considering that the S-h-rGO film was ~8.5 nm thick (Fig. 1f), about one in every 25 carbon atoms was functionalized with a sulfo group.

Fig. 1d depicts the Raman spectra of h-rGO and S-h-rGO films. The D and 2D bands exhibited small shifts after modification of the surface of the h-rGO film with sulfo groups. The D band reveals the structural defects of graphene lattice.[23, 38] These small shifts were caused by the attachment of sulfo functional groups on the carbon basal plane, and suggest that electronic transfer occurred from h-rGO to the sulfo group.[38-40] The intensity ratio of the D band to the G band for the S-h-rGO film is 0.83, which is lower than that of the h-rGO film (0.88). This reveals that the restoration of π-conjugated structures during high-temperature reduction were partly prevented by modification with functional groups.[23]

The h-rGO film was obtained by reducing an ultrathin GO film at high temperature (950 °C). The thickness of the h-rGO film could be precisely controlled from 1 to 10 nm by changing the concentration of the GO solution and spin-coating speed. We previously reported that an ~8-nm-thick h-rGO film is the most sensitive in detection.[28] After surface modification with sulfo groups, a 8.5-nm-thick S-h-rGO film was obtained. AFM images of this film are shown in Fig.1e and

Analyst Accepted Manuscript

This journal is © The Royal Society of Chemistry 2016

Please do not adjust margins

f. The right half of the image in Fig. 1e is the film, and the left half is the bare quartz plate exposed after partial removal of the film. The ultrathin S-h-rGO film has a low surface roughness of 2.69 nm (see Supplementary Information, Figure S1), making it suitable for optical sensing applications.

Detection principle

We found that graphene exhibits different reflectance in TE and TM modes under total internal reflection conditions, which is highly sensitive to the gas molecules in contact with the surface of graphene. In our previous researches[28-31], the polarization absorption effect of graphene can be described by a sandwiched graphene model as shown in Figure 2a, in which graphene layer inserted between a low-index medium (refractive index n_1, gas) and a high-index medium (refractive index n_2, SiO_2). The reflected coupling structure greatly enhances the interaction between light and the interface of graphene and gas, leading to a strong absorption difference between the TM mode and TE mode. And the difference between the reflectance of the TM mode and TE mode is the sensitivity to variations in the refractive index (RI) n_1 (gas) under the fixed conditions n_2 (SiO_2). By controlling the thickness of graphene and the incident angle, the resolution and sensitivity of the sensor can be further improved.[28]

The high sensitivity may be caused by the following characteristics of graphene. First, graphene is a two-dimensional material, and the electrons exposed on its surface are sensitive to surface changes.[7] Second, graphene is a zero-bandgap semiconductor, exhibiting strong broadband optical absorption.[41,42] Third, a reflected coupling structure greatly enhances the interaction between light and the interface of graphene and gas molecules.[28-31]

The theoretical model of the optical RI sensing is constructed on the prism/graphene film/gas three-layer structure by transfer matrix theory, and more details were previously reported by us.[28-30] In this theory, graphene is considered to be a film with a specific RI ($\hat{\mathbf{n}} = \mathbf{2.6 + 1.25i}$) and thickness, and the gas flow and adsorption processes were considered to represent the RI changes in gas layer. Gas molecules adsorbed on the surface of graphene film increased with the accumulation of time, and the equivalent RI of gas layer increased. After chemically modifying the surface of the graphene film with sulfo groups, NO_2 adsorption capacity of the sensor was enhanced, and the equivalent RI of gas layer increased faster than that without modification.

In our reported literature[28], light coupling into gas layer has a penetration depth of 2.5 μm. The equivalent RI of gas layer detected by the sensor is an average refractive index in the depth of 2.5μm. Thus, the detection signals are altered by the following two factors: (a) a change in the concentration of the upper gas molecules within the detection depth (~2.5 μm);[28] and (b) a change in the concentration of surface-adsorbed gas molecules that interact with graphene or chemically modified graphene. During the experiment, a continuous gas flow with a controlled concentration and low speed was provided to the system to minimize the change of concentration of the upper gas molecules (Fig. 2b).

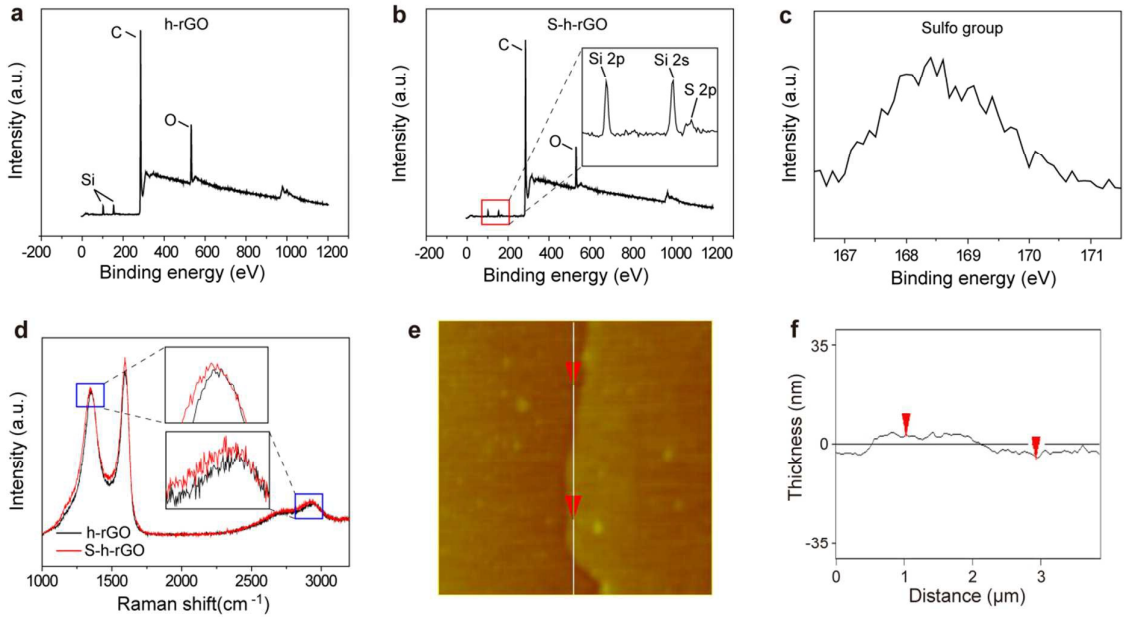

Fig. 1 Characterization of h-rGO and S-h-rGO films: (a) XPS analysis of a h-rGO film revealing the presence of the elements C (~284.77 eV), O (~532.57 eV), and Si (2p, ~102.02 eV and 2s, ~152 eV) in the film. (b) XPS analysis of a S-h-rGO film showing the presence of the elements C (~284.77 eV), O (~532.57 eV), Si (2p, ~102.02 eV and 2s, ~152 eV) and S (~168.5 eV) in the film. (c) High-resolution XPS analysis the S region (~168.5 eV) of a S-h-rGO film. (d) Raman spectra of h-rGO and S-h-rGO films. The insets are the enlarged regions of the D and 2D bands. (e) and (f) AFM characterizations of a S-h-rGO film.

Analyst Accepted Manuscript

Please do not adjust margins

Analyst

ARTICLE

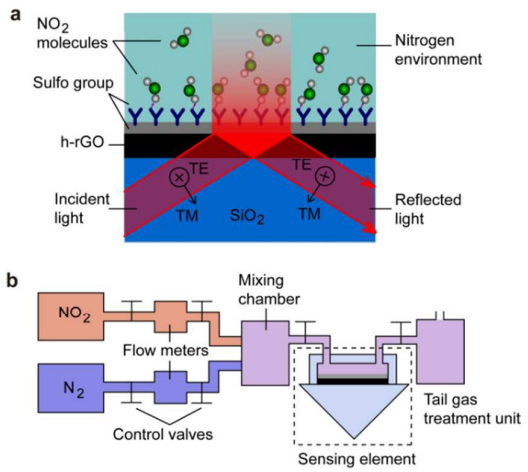

Fig. 2 Schematic diagram of the sensor and experimental setup: (a) Schematic diagram of the optical gas sensor. (b) The gas control and sensing units used in the NO_2 gas sensor.

Performance of h-rGO and S-h-rGO sensors

The intensity difference of the reflected light between TM and TE modes was captured by a balanced photoelectric detector which output a real-time voltage signal. Thus, the voltage signals were used to evaluate the performance of the novel optical gas sensor, which is more intuitive than the reflectance difference between TM and TE modes. High-purity N_2 (99.9%) was used as the load gas for a controlled concentration of NO_2 at a fixed incident light power of 0.2 mW. Fig. 3a, b and c display time-resolved voltage signals obtained for h-rGO and S-h-rGO sensors at NO_2 concentrations of 15, 50 and 100 ppm, respectively. All concentrations of NO_2 were detected by both h-rGO and S-h-rGO sensors with large signal responses, and both of the sensors show unsaturated responses after 5000 s. Compared with the h-rGO sensor, the response of the S-h-rGO sensor was much greater. Although signal responses continuously increased over time, that is, they were unsaturated, we controlled the sensing time to 600 s to aid comparison, as shown in the insets in Fig. 3a–c.

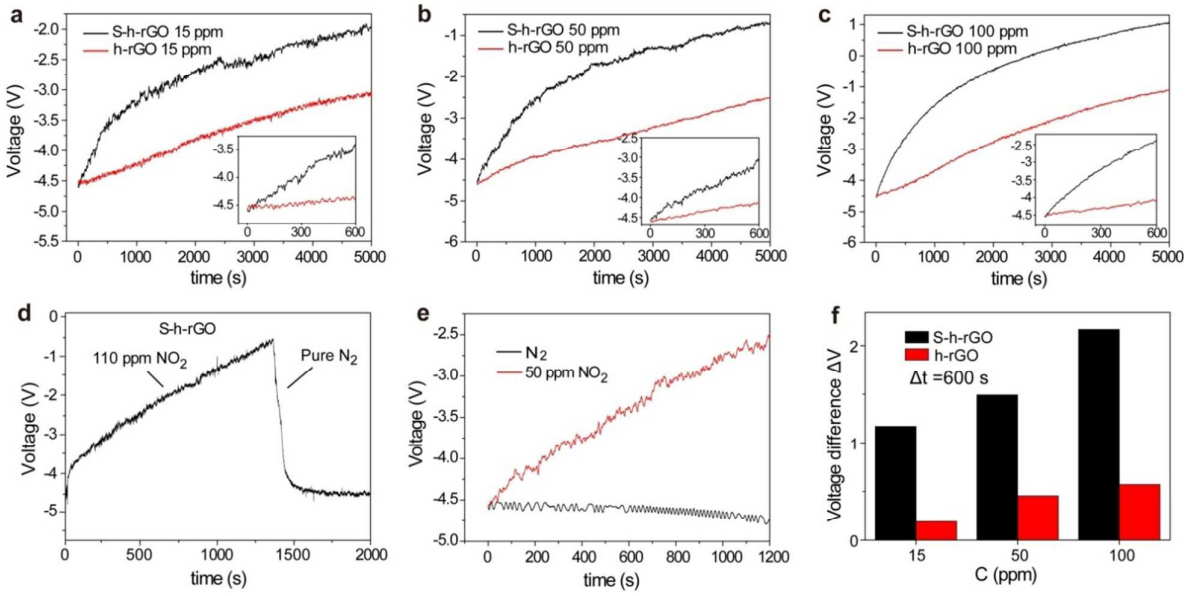

Fig. 3 Sensing and analysis results for h-rGO and S-h-rGO sensors: (a)-(c) Time-resolved voltage signals for h-rGO and S-h-rGO sensors exposed to different concentrations of NO_2 (15, 50 and 100 ppm). (d) Reversibility of the S-h-rGO sensor. (e) Responses of the S-h-rGO sensor to pure N_2 and 50 ppm NO_2. (f) Statistical results for the responses of h-rGO and S-h-rGO sensors to different concentration of NO_2 (15, 50 and 100 ppm) over 600s.

Analyst Accepted Manuscript

Please do not adjust margins

Analyst

ARTICLE

The detection limit and the sensitivity are the basic parameters of the detector.[43-45] They were evaluated based on the signal-to-noise ratio (SNR) of the maximum response at 600 s, and the formula was shown as below:

$$R_m = V_{noise} / S_m \quad (1)$$

$$S_m = M / C \quad (2)$$

where R_m is the detection limit (resolution based on maximum response analysis method); V_{noise} is the noise signal; S_m is the sensitivity; M is the maximum response and C is the concentration of NO_2 gas. Towards 15 ppm NO_2, the maximum response of the h-rGO and S-h-rGO sensors at 600 s are 0.191 and 1.171 V, respectively. The noise signal is 60 mV. Based on Eq. 1 and Eq. 2, the detection limits of the h-rGO and S-h-rGO sensors are 4.7 and 0.77 ppm, respectively, and corresponding sensitivities are 12.7 and 78 mV/ppm respectively. Thus, surface modification of the h-rGO film with sulfo groups increased the response of the sensor by about 6.1 times.

The S-h-rGO sensor exhibits superior performance to that of the h-rGO sensor for NO_2 gas sensing, which can be attributed to the following factors. The increase of Gas molecules, which are adsorbed on the graphene film surface with the accumulation of time, leads to the increase of equivalent RI of gas layer. After chemical treatment, by using sulfo groups modification on the graphene film surface, NO_2 adsorption capacity can be further enhanced, and the equivalent RI of gas layer increased faster than that without modification.

The reversibility experiment of the sensor was implemented, and the corresponding result is shown in the Figure 3d. The result shows that we send 110 ppm NO_2 gas (N_2 as the carrier gas), and the output voltage signal increases. After 1300 s, we send the carrier gas (pure N_2) the output voltage signal can be recovered rapidly. It demonstrates that the sensor has a good reversibility. The effect of the N_2 carrier gas on the sensor signal needs to be measured. Fig. 3e illustrates the responses of the S-h-rGO sensor to pure N_2 and 50 ppm NO_2 in N_2. Compared with 50 ppm NO_2, the response to pure N_2 is almost constant, and even has a downward trend. This may be caused by the gas adsorbed on the surface of the S-h-rGO film during sample preparation being desorbed by the N_2 gas flow. Based on maximum value analysis, the statistical results for the h-rGO and S-h-rGO sensors with different concentration of NO_2 were on display, as shown in Fig. 3f. Compared with the h-rGO sensor, the response of the S-h-rGO sensor was greatly enhanced after 600 s under different concentrations of NO_2.

Sensing results for S-h-rGO sensor based on initial slope analysis

The analysis method based on the saturated maximum response is widely used in gas sensors.[7, 11-23] However, to obtain a saturated response, a long accumulation period is required, which highlights the inverse relationship between sensitivity and response time. Because the adsorption and exchange of gas molecules occurred on the surface of S-h-rGO film, the changes of equivalent RI of gas layer can only be caused by chemical or physical adsorption instead of gas permeability. Here we propose an analysis method based on the slopes of the initial responses of the novel gas sensors. The initial responses (up to 300 s) and linear fitting curves of the S-h-rGO sensor to different concentrations of NO_2 (15, 50, 80, 100 and 115 ppm) are shown in Fig. 4a. The initial responses show consistent linear growth over this period. And their linear fitting curves indicate that the slope of the curves increases with the concentration of NO_2. Thus, the slope k was used as a parameter to measure the signal responses of the sensors. Slope analysis using different time periods and different concentrations of NO_2 is depicted in Fig. 4b. The results clearly reveal that the signal responses based on the initial slope analysis decreased over time. This means that the shorter the sensing time, the greater the relative signal response. Unlike the analysis of saturated response, using the initial slope analysis overcomes the issue of the inverse relationship between sensitivity and response time. In the analysis results in Fig. 4b, large slope changes were obtained during the first tens of seconds of exposure of the sensor to NO_2 gas, and after 120s, the slopes began to stabilize. Upon exposure to NO_2 gas for 300 s, towards 15 ppm NO_2 the slope change Δk over the 60 s from 240 to 300 s was 2×10^{-5}. Relative to the slope at 300 s, k_{300} = 1.1×10^{-3}, the rate of change $\Delta k / k_{300}$ over the 60 s from 240 to 300 s is less than 2%, which is close to the detection limit of the S-h-rGO sensor evaluated below. Thus, the slope responses at 300 s were used in the analysis.

The statistical results determined by the initial slope analysis for the S-h-rGO sensor toward different concentrations of NO_2 are presented in Fig. 4c. Compared with the maximum response analysis (Fig. 3f), the response of the S-h-rGO sensor was greatly improved by using the initial slope analysis and the response was obtained in a shorter period of time. Fig. 4d shows the detection limits of the S-h-rGO sensor evaluated with different concentrations of NO_2 based on the initial slope analysis. The initial responses show consistent linear growth over 300 s, thus, the initial slope response around 300s was considered as a constant value. Using the slope analysis method, the detection limit and sensitivity were evaluated based on the slope-to-uncertainty ratio within 300 s and the formula was shown as below:

$$R_k = U_k / S_k \quad (3)$$

$$S_k = k / C \quad (4)$$

Analyst Accepted Manuscript

This journal is © The Royal Society of Chemistry 2016

Please do not adjust margins

Analyst

ARTICLE

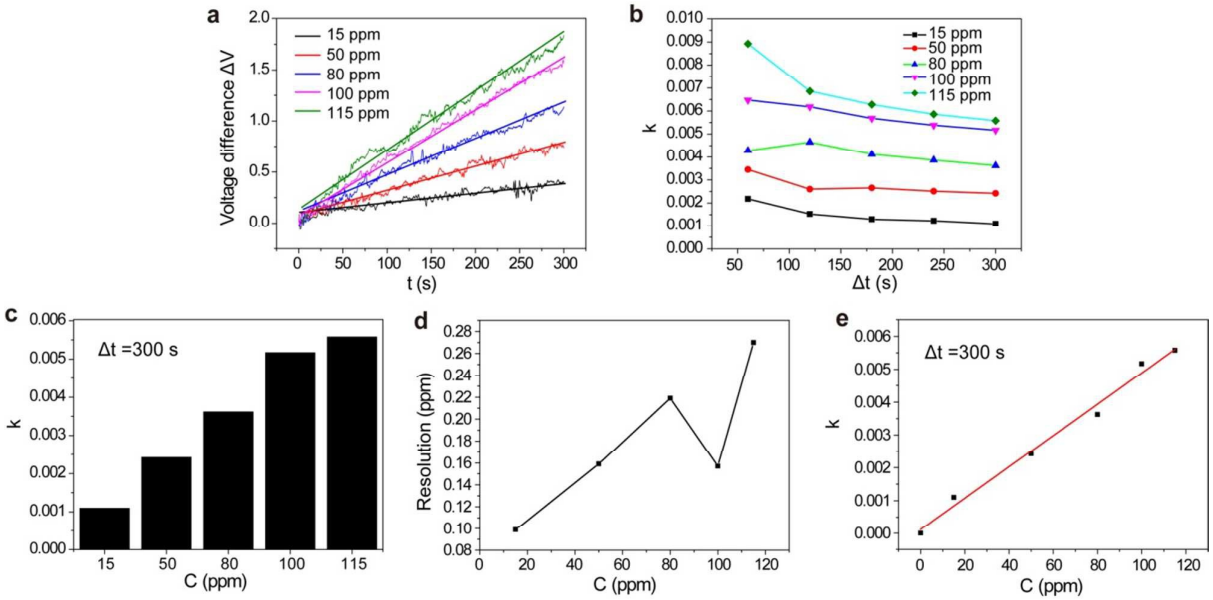

Fig. 4 Sensing results for the S-h-rGO sensor based on initial slope analysis: (a) Initial responses (up to 300 s) and linear fitting curves of the S-h-rGO sensor to different concentrations of NO_2 (15, 50, 80, 100 and 115 ppm). Linear fitting curves obtained with the least square method. (b) Slope analysis using different time periods (60, 120, 180, 240 and 300 s) for different concentrations of NO_2 (15, 50, 80, 100 and 115 ppm).(c) Statistical results for the initial slope of the S-h-rGO sensor with different concentrations of NO_2 (15, 50, 80, 100 and 115 ppm) over 300 s. (d) Detection limits of the S-h-rGO sensor evaluated with different concentrations of NO_2 (15, 50, 80, 100 and 115 ppm) over 300 s. (e) Linearity measurements.

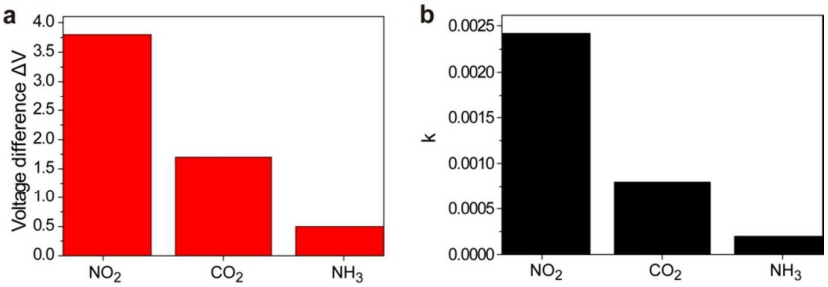

Fig. 5 Selectivity of the S-h-rGO sensor for different interference gases (CO_2 and NH_3): (a) Selectivity based on saturated response analysis. (b) Selectivity based on initial slope analysis.

where R_k and S_k are the detection limit and the sensitivity based on slope analysis method; U_k is the uncertainty of the slope; k is the slope response within 300 s and C is the concentration of NO_2 gas. Towards 15 ppm NO_2, the slope of the S-h-rGO sensors within 300 s is 0.0011, and the uncertainty of the slope is 7.26×10^{-6}, thus, based on Eq. 3 and Eq. 4, the detection limit of the S-h-rGO sensor is 0.099 ppm. In order to reduce the estimation error caused by a single concentration, more concentrations were used to evaluate the detection limits, including 50 ppm, 80 ppm, 100 ppm and 110 ppm. Among them, the maximum value of 0.28 ppm was considered as the detection limit within 100 ppm.

Linearity is another important indicator of sensors that is measured in this work. The experimental (points) and fitting results (line) for initial slope analysis are displayed in Fig. 4e. The results show good linearity for NO_2 concentrations within 100 ppm. The

Analyst Accepted Manuscript

Please do not adjust margins

slope k increased with concentration of NO_2 gas C, and the linear relationship is given by:

$$k = 4.82 \times 10^{-5} C - 9.01 \times 10^{-5} \quad (5)$$

Selectivity of the S-h-rGO sensor

The selectivity of the S-h-rGO sensor was investigated by measuring the responses of the sensor towards other gases including CO_2 and NH_3, in terms of maximum value after 600 s (Fig. 5a) and initial slope after 300 s (Fig. 5b). The concentration of the gases, including NO_2, CO_2 and NH_3, is 50 ppm. The S-h-rGO sensor exhibited excellent selectivity for NO_2 gas. Furthermore, compared with the maximum response analysis, the selectivity of the S-h-rGO sensor was improved by using the initial slope analysis method.

Conclusions

We developed a novel high-performance NO_2 gas sensor based on a h-rGO film chemically modified with sulfo groups. The sensor combined the advantages of electrochemical and optical sensing, including fast response, high sensitivity and resolution, good linearity, reversibility and selectivity, detection at room temperature and atmospheric pressure, non-contact, low cost and safety. The response of the S-h-rGO sensor was about 6.1 times higher than that of the h-rGO sensor. Based on the traditional analysis method, the detection limits of the h-rGO and S-h-rGO sensors are 4.7 and 0.77 ppm, respectively, and corresponding sensitivities are up to 12.7 and 78 mV/ppm, respectively. Because of the characteristics of the chemically modified h-rGO film, particularly impermeable adsorption and exchange of gas molecules, we proposed an analysis method using the initial slope of the sensor response. Using the developed initial slope analysis method, the issues caused by the inverse relationship between sensitivity and response time in the saturated response analysis were solved. In addition, the resolution, linearity and selectivity of the sensor were further improved using the initial slope analysis. Currently, this analysis method cannot be used to measure the concentrations of NO_2 gas in an unknown gas environment but, considering the advantages of the slope analysis method described above, this analysis method is worthy of being adopted for gas sensing. And this work indicates that surface chemical modification of films is an effective approach to improve the performance of sensors, and opens a new door to realize high-performance optical gas sensors.

Acknowledgements

This work was partially supported by the National Nature Science Foundation of China under Grant Nos. 61138003, 61427819, 61505109, 61405121 and 61377052; Ministry of Science and Technology of China under National Basic Research Program of China (973) grant No.2015CB352004; China Postdoctoral Science Foundation (2015M570721) , Science and Technology Innovation Commission of Shenzhen under grant Nos. KQCS2015032416183980, CYJ20140418091413543; Natural Science Foundation of SZU (Grant No. 201454) and the start-up funding of SZU (000011, 000075), and the start-up funding at Shenzhen University.

Notes and references

1 B. Yu, F. Zhai, H. Cong and D. Yang, *Journal of Materials Chemistry C*, 2016, **4**, 1386-1391.
2 X. Wang, F. Sun, Y. Duan, Z. Yin, W. Luo, Y. Huang and J. Chen, *Journal of Materials Chemistry C*, 2015, **3**, 11397-11405.
3 J. Gong, Y. Li, Z. Hu, Z. Zhou and Y. Deng, *The Journal of Physical Chemistry C*, 2010, **114**, 9970–9974.
4 X. Yu, Y. Li, J. Cheng, Z. Liu, Q. Li, W. Li, X. Yang and B. Xiao, *ACS applied materials & interfaces*, 2015, **7**, 13707–13713.
5 Y. K. Mishra, G. Modi, V. Cretu, V. Postica, O. Lupan, T. Reimer, I. Paulowicz, V. Hrkac, W. Benecke, L. Kienle and R. Adelung, *ACS applied materials & interfaces,* 2015, **7**, 14303–14316.
6 S. Yang, Z. Wang, Y. Hu, X. Luo, J. Lei, D. Zhou, L. Fei, Y. Wang and H. Gu, *ACS applied materials & interfaces*, 2015, **7**, 9247–9253.
7 F. Schedin, A. K. Geim, S. V. Morozov, E. W. Hill, P. Blake, M. I. Katsnelson and K. S. Novoselov, *Nature materials*, 2007, **6**, 652–655.
8 H. J. Yoon, J. H. Yang, Z. Zhou, S. S. Yang and M. M. C. Cheng, *Sensors and Actuators B: Chemical*, 2011, **157**, 310–313.
9 G. Singh, A. Choudhary, D. Haranath, A. G. Joshi, N. Singh, S. Singh and R. Pasricha, *Carbon*, 2012, **50**, 385–394.
10 J. D. Fowler, M. J. Allen, V. C. Tung, Y. Yang, R. B. Kaner and B. H. Weiller, *Acs Nano*, 2009, **3**, 301–306.
11 N. Tammanoon, A. Wisitsoraat, C. Sriprachuabwong, D. Phokharatkul, A. Tuantranont, S. Phanichphant and C. Liewhiran, *ACS applied materials & interfaces*, 2015, **7**, 24338–24352.
12 Y. Dan, Y. Lu, N. J. Kybert, Z. Luo and A. C. Johnson, *Nano Letters*, 2009, **9**, 1472–1475.
13 H. E. Romero, P. Joshi, A. K. Gupta, H. R. Gutierrez, M. W. Cole, S. A. Tadigadapa and P. C. Eklund, *Nanotechnology*, 2009, **20**, 245501.
14 R. Pearce, T. Iakimov, M. Andersson, L. Hultman, A. L. Spetz and R. Yakimova, *Sensors and Actuators B: Chemical*, 2011, **155**, 451–455.
15 A. Salehi, D. Estrada, K. Y. Lin, M. H. Bae, F. Xiong, E. Pop, R. I. Masel, *Advanced materials*, 2012, **24**, 53–57.
16 K. Yu, P. Wang, G. Lu, K. H. Chen, Z. Bo and J. Chen, *The Journal of Physical Chemistry Letters*, 2011, **2**, 537–542.
17 W. Li, X. Geng, Y. Guo, J. Rong, Y. Gong, L. Wu, X. Zhang, P. Li, J. Xu, G. Cheng, M. Sun and L. Liu, *ACS nano*, 2011, **5**, 6955–6961.
18 X. An, C. Y. Jimmy, Y. Wang, Y. Hu, X. Yu and G. Zhang, *Journal of Materials Chemistry*, 2012, **22**, 8525-8531.
19 S. Mao, S. Cui, G. Lu, K. Yu, Z. Wen and J. Chen, *Journal of Materials Chemistry*, 2012, **22**, 11009-11013.
20 F. Yavari, Z. Chen, A. V. Thomas, W. Ren, H. M. Cheng and N. Koratkar, *Scientific reports*, 2011, **1**.
21 K. H. Cheon, J. Cho, Y. H. Kim and D. S. Chung, *ACS applied materials & interfaces*, 2015, **7**, 14004–14010.
22 J. Wu, K. Tao, J. Miao and L. K. Norford, *ACS applied materials & interfaces*, 2015, **7**, 27502–27510.
23 W. Yuan, A. Liu, L. Huang, C. Li and G. Shi, *Advanced Materials*, 2013, **25**, 766–771.
24 S. A. Kolpakov, N. T. Gordon, C. Mou and K. Zhou, *Sensors*, 2014, **14**, 3986–4013.

Analyst Accepted Manuscript

Please do not adjust margins

25 G. Mattei, P. Mazzoldi, M. L. Post, D. Buso, M. Guglielmi and A. *Advanced Materials*, 2007, **19**, 561–564.
26 V. Spagnolo, A. A. Kosterev, L. Dong, R. Lewicki, F. K. Tittel, *Applied Physics B*, 2010, **100**, 125–130.
27 A. Paliwal, A. Sharma, M. Tomar and V. Gupta, *Sensors and Actuators B: Chemical*, 2015, **216**, 497–503.
28 F. Xing, G. X. Meng, Q. Zhang, L. T. Pan, P. Wang, Z. B. Liu, W. S. Jiang, Y. S. Chen and J. G. Tian, *Nano Letters*, 2014, **14l**, 3563–3569.
29 F. Xing, Z. B. Liu, Z. C. Deng, X. T. Kong, X. Q. Yan, X. D. Chen, Q. Ye, C. P. Zhang, Y. S. Chen and J. G. Tian, *Scientific reports*, 2012, **2**, 908.
30 Q. Ye, J. Wang, Z. B. Liu, Z. C. Deng, X. T. Kong, F. Xing, X. D. Chen, W. Y. Zhou, C. P. Zhang and J. Tian, *Appl. Phys. Lett.*, 2013, **102**, 021912.
31 F. Xing, W. Xin, W. S. Jiang, Z. B. Liu and J. G. Tian, *Applied Physics Letters*, 2015, **107**, 163110.
32 W. S. Hummers Jr and R. E. Offeman, *Journal of the American Chemical Society*, 1958, **80**, 1339–1339.
33 L. Zhang, J. Liang and Y. Huang, *Carbon*, 2009, **47**, 3365–3368.
34 Y. Si and E. T. Samulski, *Nano letters*, 2008, **8**, 1679–1682.
35 J. W. Park, B. Vahidi, A. M. Taylor, S. W. Rhee and N. L. Jeon, *Nature protocols*, 2006, **1**, 2128–2136.
36 G. Bar, L. Delineau, A. Häfele, M. H. Whangbo, *Polymer*, 2001, **42**, 3627-3632.
37 K. S. Houston, D. H. Weinkauf, F. F. Stewart, *Journal of Membrane Science*, 2002, **205**, 103-112.
38 K. Krishnamoorthy, M. Veerapandian, R. Mohan and S. J. Kim, *Applied Physics A*, 2012, **106**, 501–506.
39 J. C. Chacon-Torres, L. Wirtz and T. Pichler, *ACS Nano*, 2013, **7**, 9249–9259.
40 A. C. Ferrari, J. C. Meyer, V. Scardaci, C. Casiraghi, M. Lazzeri, F. Mauri, S. Piscanec, D. Jiang, K. S. Novoselov, S. Roth and A. K. Geim, *Physical review letters*, 2006, **97**, 187401.
41 F. Bonaccorso, Z. Sun, T. Hasan, A. C. Ferrari, *Nat. Photonics*, 2010, **4**, 611–622.
42 Q. Bao and K. P. Loh, *ACS Nano*, 2012, **6**, 3677–3694.
43 A. D'Amico, C. Di Natale, *IEEE Sens. J.*, 2001, **1**, 183-190.
44 Q. Huang, D. Zeng, H. Li, C. Xie, *Nanoscale*, 2012, **4**, 5651-5658.
45 A. Sharma, M. Tomar and V. Gupta, *Journal of Materials Chemistry*, 2012, **22**, 23608-23616.

Analyst Accepted Manuscript

This journal is © The Royal Society of Chemistry 2016

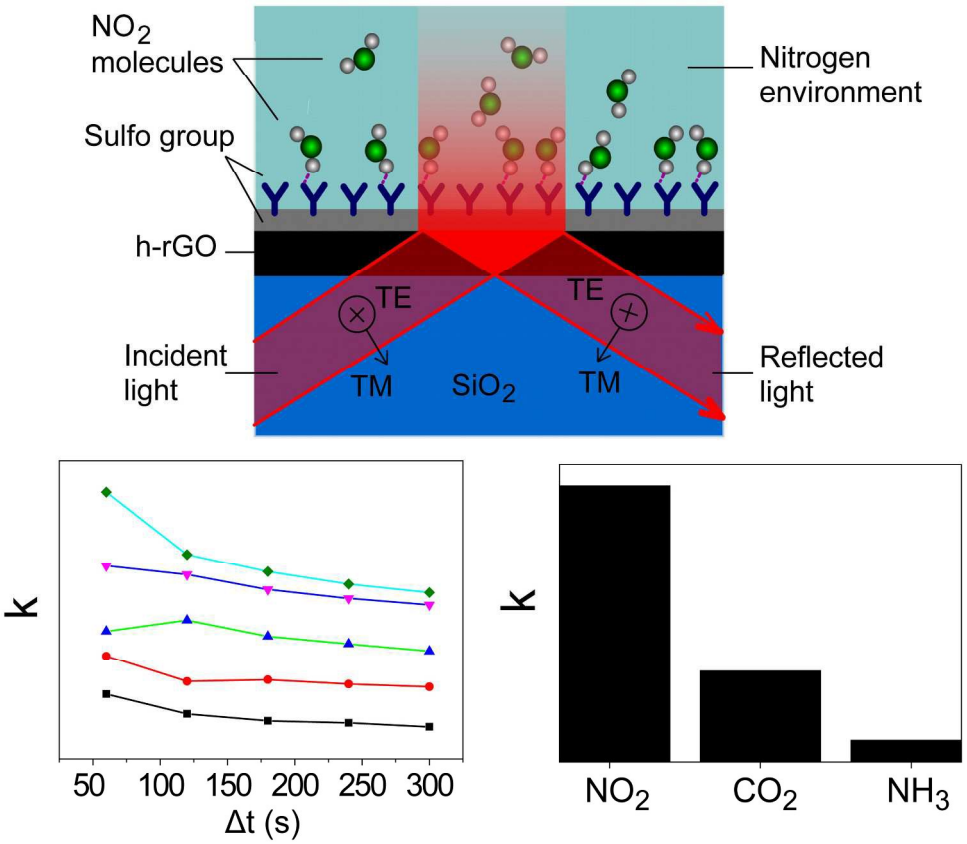

212x186mm (300 x 300 DPI)

Analyst Accepted Manuscript